



Antimicrobial activity of amphiphilic neamine derivatives: Understanding the mechanism of action on Gram-positive bacteria

Jitendriya Swain^a, Micheline El Khoury^a, Aurélien Flament^a, Clément Dezanet^b, Florian Briée^b, Patrick Van Der Smissen^c, Jean-Luc Décout^b, Marie-Paule Mingeot-Leclercq^{a,*}

^a Université catholique de Louvain, Louvain Drug Research Institute, Pharmacologie Cellulaire et Moléculaire, avenue E. Mounier 73, UCL B1.73.05, 1200 Brussels, Belgium

^b Université Grenoble Alpes/CNRS, Département de Pharmacochimie Moléculaire, rue de la Chimie, F-38041 Grenoble, France

^c Université catholique de Louvain, de Duve Institute, avenue Hippocrate 75, UCL B1.75.05, 1200, Brussels, Belgium

ARTICLE INFO

Keywords:

Bacterial membranes
Antibiotics
Amphiphilic aminoglycosides
Gram-positive
S. aureus
B. subtilis
Lipoteichoic acid
Cardiolipin
Membrane permeability
Membrane depolarization

ABSTRACT

Amphiphilic aminoglycoside derivatives are potential new antimicrobial agents mostly developed to fight resistant bacteria. The mechanism of action of the 3',6-dinonyl neamine, one of the most promising derivative, has been investigated on Gram-negative bacteria, including *P. aeruginosa*. In this study, we have assessed its mechanism of action against Gram-positive bacteria, *S. aureus* and *B. subtilis*. By conducting time killing experiments, we assessed the bactericidal effect induced by 3',6-dinonyl neamine on *S. aureus* MSSA and MRSA. By measuring the displacement of BODIPYTM-TR cadaverine bound to lipoteichoic acids (LTA), we showed that 3',6-dinonyl neamine interacts with these bacterial surface components. We also highlighted the ability of 3',6-dinonyl neamine to enhance membrane depolarization and induce membrane permeability, by using fluorescent probes, DiSC₃C(5) and propidium iodide, respectively. These effects are observed for both MSSA and MRSA *S. aureus* as well as for *B. subtilis*. By electronic microscopy, we imaged the disruption of membrane integrity of the bacterial cell wall and by fluorescence microscopy, we demonstrated changes in the localization of lipids from the enriched-septum region and the impairment of the formation of septum. At a glance, we demonstrated that 3',6-dinonyl neamine interferes with multiple targets suggesting a low ability of bacteria to acquire resistance to this agent. In turn, the amphiphilic neamine derivatives are promising candidates for development as novel multitarget therapeutic antibiotics.

1. Introduction

Bacteria have distinct cell body shapes, ranging from spheres (cocci) to rods (bacilli) as for *S. aureus* and *B. subtilis* in Gram-positive bacteria. Their mode of growth and division is also very diverse with temporal and spatial modifications in lipid composition of bacterial membranes upon changes in lipid environment [1] and ability of lipids to form subdomains of unique protein and lipid composition. This can influence membrane protein organization and/or function, providing a further control level for regulating protein function within a membrane [2]. Understanding how lipids and proteins interplay for proper functionality of bacterial membranes and how new drugs might affect this interplay can open new avenues in the search for new antibiotics. In this context, molecules able to interact with lipids and alter the biophysical properties of bacterial lipid membranes, which in turn can modulate protein activity [3,4], are more and more investigated. Pursuing this

approach, amphiphilic aminoglycosides namely neamine derivatives have been synthesized by the team of Decout [5–9]. The neamine core is made of a moiety of the neomycin B antibiotic composed of the aminoglucosamine and 2-deoxystreptamine ring carrying four amino groups which can be protonated at physiological pH. The amphiphilic character results from grafting of two lipophilic groups on the neamine core. Both of them can be grafted on the same aminoglucosamine ring (3',4'-dialkyl neamine derivatives) or one on each ring (3',6-dialkyl neamine derivatives).

Activity/toxicity relationship delineation has been done on >90 derivatives [5,7–9]. One of the most promising derivatives, the 3',6-dinonyl neamine (Fig. 1), is active against a large variety of bacteria, including Gram-negative and Gram-positive bacteria, susceptible and resistant strains, laboratory and clinical strains [5,7,8]. So far, detailed studies of the antimicrobial activity and the molecular mechanism of action of 3',6-dinonyl neamine have been done on Gram-negative

* Corresponding author.

E-mail address: marie-paule.mingeot@uclouvain.be (M.-P. Mingeot-Leclercq).

<https://doi.org/10.1016/j.bbamem.2019.05.020>

Received 2 December 2018; Received in revised form 22 May 2019; Accepted 28 May 2019

Available online 31 May 2019

0005-2736/ © 2019 Published by Elsevier B.V.

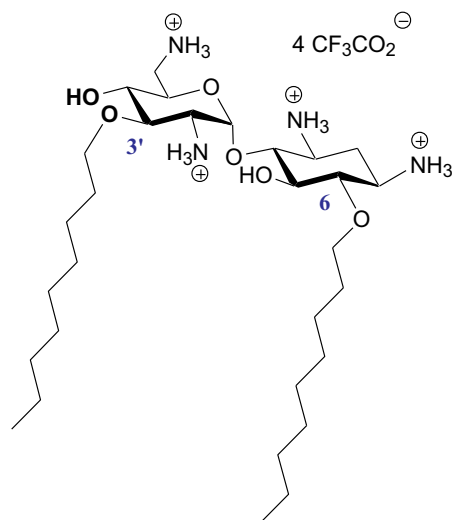


Fig. 1. Structure of 3',6-dinonyl neamine.

bacteria, including on *P. aeruginosa* [10–13]. In addition to low MICs values, the exposure of *P. aeruginosa* ATCC 27853 to the 3',6-dinonyl derivative over one month at the half-MIC, only slightly increases the MIC value (from 1 to 4 mg/mL) as compared to MIC values measured for ciprofloxacin which increased faster and in a higher extent (from 0.5 to 32 µg/mL) [9]. 3',6-Dinonyl neamine also shows ability to inhibit biofilm formation [11]. By using membrane model systems and bacteria (*P. aeruginosa*), we demonstrated the interaction of 3',6-dinonyl neamine with outer membrane lipopolysaccharides [11] and inner membrane anionic phospholipids mostly cardiolipin leading to membrane permeabilization and depolarization [12]. By targeting cardiolipin-bacterial microdomains mainly located at the cell poles, 3',6-dinonyl neamine leads to disassembly these microdomains into cardiolipin clusters and relocation of cardiolipin domains [13]. Importantly, targeting cardiolipin-lipid domains results in bacterial morphological changes. These changes are characterized by a severe length decrease probably as a result from the decrease of the inner membrane fluidity/hydration which could impair the dynamics of cell-shape determining proteins like MreB [13].

On Gram-positive bacteria, despite interesting antimicrobial activity of 3',6-dinonyl neamine on *S. aureus* MRSA or VRSA [7,8], data on its potential mechanism and effect on the biophysical properties of lipid membranes in relation with critical events like the bacterial cell division and peptidoglycan synthesis are lacking.

Gram-positive bacteria differ from Gram-negative bacteria in many ways, including the structure and composition of their lipid membranes. The envelope of Gram-positive bacteria consists of the cell wall and the cytoplasmic membrane. The cell wall is composed of a thick peptidoglycan layer in which anionic polymers teichoic acids (60–70% mass of cell wall) are surrounded. In addition to the teichoic acids, the cell wall of Gram-positive bacteria is decorated with a variety of proteins. Interestingly, cardiolipin (CL) (5–25%) is also present in Gram-positive bacteria with phosphatidylglycerol (PG) (60–70%), phosphatidylethanolamine (PE) (10–20%), and andlyosphosphatidylglycerol (LPG) (15–40%) [14,15]. Globally, anionic lipids like CL, PG, and LPG constitute >80% of the total lipid found in the membranes of Gram-positive bacteria but <30% of the lipid present in those of Gram-negative bacteria [16]. In addition to the lipid components, the cell membrane of Gram-positive bacteria contains the lipid anchor component of lipoteichoic acid (LTA) [17].

The aim of this work is to decipher the mechanism involved in the activity of 3',6-dinonyl neamine on Gram-positive bacteria. We selected *Staphylococcus aureus* ATCC 25923 as an example of cocci and *Bacillus subtilis* ATCC 6633 as a model of rod-shaped bacteria. *S. aureus* may

cause bloodstream, lower respiratory tract, skin and soft tissue infections inflicting high morbidity and mortality worldwide, mostly due to its ability to acquire resistance to antimicrobial agents [18]. Thus, for some selected experiments, we also used MRSA strains (ATCC 33591, ATCC 33592 or COL). *B. subtilis* is considered as the principal Gram-positive model organism with specific characteristics including the existence of lipid domains smaller than 40 nm [19] and a greater thickness of cell wall as compared with other Gram-positive bacteria.

We first investigated the potential bactericidal/bacteriostatic effect of 3',6-dinonyl neamine by determining the killing curves. Second, we explored the ability of 3',6-dinonyl neamine to interact with lipoteichoic acids by measuring the displacement of BODIPY™-TR cadaverine bound to LTA, and to induce changes in membrane potential and membrane permeabilization as determined by using fluorescent probes, DiSC₃C(5) and propidium iodide, respectively. Third, we imaged morphological changes of bacterial cells treated with 3',6-dinonyl neamine by electron microscopy. Fourth, to decipher a potential effect on bacterial division and/or peptidoglycan synthesis, we characterized the effect induced by 3',6-dinonyl neamine by imaging PBP2 (GFP-PBP2), a septum localized protein involved in *S. aureus* division. We also visualized lipids (Nile Red Fluorescence) as the mirror of MreB, a cell shape-determining bacterial actin homologue which might serve as an organizer or tracking device for the PBP2-peptidoglycan biosynthesis complex [20]. All these effects give insight about the mechanism of action of 3',6-dinonyl neamine on Gram-positive bacteria, including *S. aureus*.

2. Experimental techniques

3',6-Dinonyl neamine was synthesized by Decout and colleagues [6,8]. Propidium iodide (PI), Nile red and DiSC₃(5) were ordered from Invitrogen (Paisley, Scotland, UK). Cell-free lipoteichoic acid (LTA) from *S. aureus* was obtained from Sigma-Aldrich. BODIPY™-TR-cadaverine [BC] was ordered from Molecular Probes (Invitrogen, Carlsbad, CA). All other analytical grade reagents were purchased from E. Merck AG.

2.1. Bacteria strains and growth conditions

Bacillus subtilis ATCC 3366, *Staphylococcus aureus* ATCC 25923, ATCC 33592, ATCC33591 (MRSA and β-lactamase producer; American Type Culture Collection, Manassas, VA, USA) and COL (HA-MRSA) were used as a reference strain [21,22]. The homogeneous MRSA strain BCBPM073, derived from COL and carrying a single copy of PBP2 with an N-terminal superfast GFP fusion [23] was used for the PBP2 localization study.

Trypticase soy agar (TSA) plate was used to grow Gram-positive bacteria at 37 °C. One colony of bacteria was suspended in Cation Adjusted –Müller Hinton Broth (Ca-MHB) and incubated overnight at 37 °C on a rotary shaker (130 rpm).

2.2. MIC determination

All strains were grown overnight at 37 °C on Trypticase soy agar (TSA) Petri dishes (BD Diagnostics, BD, Franklin Lakes, NJ). Minimal Inhibitory Concentrations (MICs) were determined by microdilution method (96 well plate) using a fresh culture of Gram-positive bacteria in cation-adjusted Mueller-Hinton broth (CA-MHB), according to the recommendations of the Clinical and Laboratory Standards Institute (CLSI).

2.3. Time-killing curves

Time-kill assays were performed according to guideline of the CLSI (2017). The antimicrobial activities of gentamicin, linezolid and 3',6-dinonyl neamine against *S. aureus* MSSA (ATCC 25923) and MRSA (ATCC 33592) were evaluated by time-kill studies with starting inocula

of 1×10^6 CFU/ml. Antibiotic concentrations at 0.25, 1, 2 and 5 the MIC of the test strain were prepared in water. Growth in the absence of antibiotics served as the control. Colony counts were determined after 0, 1, 3, 5 and 8 h of incubation at 37 °C by plating aliquots of appropriate dilutions on Trypticase Soy Agar (TSA). If required, 10-fold dilutions were performed allowing accurate colony counts in the range of 10 to 250 CFU per plate and minimization of the effects of drug carryover. The quantification limit was set equal to a reduction to -5 in the \log_{10} CFU/ml (Δ Log CFU (8 h–0 h)).

2.4. BODIPYTM-TR-cadaverine displacement assay

Binding affinity to lipoteichoic acid (LTA) from *S. aureus* was investigated in a cell free system as well as on bacteria, by using BODIPYTM-TR-cadaverine displacement assay. Quenching of fluorescence intensity was observed when probe bound to LTA. Displacement of probe into the solution leads to enhancement of its fluorescence [24,25]. The assays were performed in 96-well plates. Fluorescence intensity was measured on a SpectraMax Gemini XS microplate spectrofluorometer using excitation and emission wavelengths of 580 nm and 620 nm, respectively.

For cell free assays, stock solutions of BODIPYTM-TR-cadaverine (10 mM) and LTA (14 µg/mL) were prepared by dissolution in Tris buffer (50 mM, pH 7.4). Desired concentration of BODIPYTM-TR-cadaverine (final concentration 5 µM) and cell-free LTA (final concentration 3.5 µg/mL) were mixed. After 15 min, selected compounds were mixed and plates were kept for 30 min in the dark at room temperature.

For experiments performed on *S. aureus* (MSSA [ATCC 25923], MRSA [ATCC 33591, COL]) and *B. subtilis* (ATCC 6633) desired concentration of BODIPYTM-TR-cadaverine and freshly grown Gram-positive bacteria (final A_{620} - 0.05) were mixed. Mixture was kept for 30 min in the dark at room temperature until equilibration. After 30 min, concentrations of the selected compounds and mixture of BODIPYTM-TR-cadaverine (final concentration 5 µM) and freshly grown Gram-positive bacteria were added to the plate and kept for 30 min.

2.5. Bacterial membrane depolarization

The changes in membrane potential of the bacteria was determined with a membrane-potential sensitive fluorescent dye DiSC₃(5) [26]. Bacteria were grown in Ca-MHB overnight at 37 °C under agitation (130 rpm). Bacterial suspension was diluted and OD₆₀₀ was monitored to reach a value of 0.3 for *S. aureus* (MSSA [ATCC 25923], MRSA [ATCC 33591, COL]) and 0.2 for *B. subtilis* (ATCC 6633) [27]. The bacteria were washed with Hepes (5 mM), glucose (5 mM), and centrifuged (300g 10 min). The pellet was resuspended in buffer containing Hepes (5 mM), Glucose (5 mM) and KCl (100 mM for *S. aureus* and 300 mM for *B. subtilis* [27]) to achieve an OD₆₀₀ of 0.05. The DiSC₃(5) probe was added (800 nM final concentration), and the bacterial suspension was incubated in the dark for 4 min at 37 °C. The fluorescence quenching was monitored until a stable signal intensity was observed. 3',6-dinonyl neamine along with other compounds of interest were then distributed in a 96-well microplate to obtain a final concentration of compound of interest ranging from 0.5 to 20 µM. The fluorescence intensity was measured at 15 min after addition of bacterial suspension with a SpectraMax-M3 microplate reader at 25 °C (Molecular Devices, Sunnyvale, CA) (excitation and emission wavelengths of 630 and 680 nm, respectively). A preliminary experiment, without bacterial cells, was performed to ensure that the presence of 3',6-dinonyl neamine and valinomycin had no effect on DiSC₃(5) fluorescence.

2.6. Bacterial membrane permeabilization

The bacterial membrane permeabilization was studied with a membrane-impermeable fluorescent dye propidium iodide (PI) [28]. The experiments were performed on *S. aureus* (MSSA [ATCC 25923],

MRSA [ATCC 33591, COL]) and *B. subtilis* (ATCC 6633). A stock solution of PI (3 mM in pure water) was diluted 100-fold with the bacterial suspension (OD₆₂₀ of 0.05). 3',6-Dinonyl neamine along with other compounds of interest, at final concentrations ranging from 1 to 7 µM, were added to the PI-containing (final concentration 30 µM) bacterial suspension in 96-well microplates. The fluorescence intensity were measured with a SpectraMax-M3 microplate reader at 25 °C after 15 min (Molecular Devices, Sunnyvale, CA) for excitation and emission wavelengths of 540 and 610 nm, respectively.

2.7. Scanning electron microscopy

S. aureus (ATCC 25923) and *B. subtilis* (ATCC 6633) were grown up to mid log (OD₆₂₀ - 0.2–0.3). Bacteria were washed in phosphate buffered saline (0.1 M PBS, pH 7.4) and then treated with 3',6-dinonyl neamine for 1 h. A suspension of bacterial cells was immobilized on poly-L-lysine coated coverslips for 10 min at room temperature. After washing in buffer - to remove the excess of free-floating bacteria- the coverslips were incubated in 1% glutaraldehyde in order to cross-link the already fixed bacteria on the poly-lysine. We further post-fixed the samples in 1% osmium tetroxide in cacodylate buffer for 2 h at 4 °C and washed extensively in water. Samples were then dehydrated in graded series of ethanol, critical point dried and coated with 10 nm of gold. Samples were observed in a CM12 Philips electron microscope at 80 kV with the secondary electron detector.

2.8. Fluorescence imaging

The fluorescence of Nile Red is highly sensitive towards nonpolar micro-environments and exhibits intense emission that are commonly used to detect and identify changes in lipid membrane properties including fluidity [29,30]. For fluorescence imaging experiments, *S. aureus* (ATCC 25923) and *B. subtilis* (ATCC 6633) cells were incubated with the membrane dye Nile Red [31] at a final concentration of 2 µg/mL, for 5 min at room temperature with agitation (500 rpm). Subsequently, the cells were placed on an agarose pad or poly-L-lysine coated coverslips for time-lapse experiment. Time-lapse experiment image sets were captured every 1 min, for a total period of 30 min. Measurements were performed on wide field fluorescence microscopy using ZEN software with 555 nm excitation laser.

For fluorescence microscopy of COL-PBP2 GFP strain, cells were grown to mid-exponential phase at 37 °C and analyzed on microscope slides covered with a thin film of agarose in PBS. The antibiotic was usually added to the bacteria (OD₆₂₀ of 0.4).

3. Results

3.1. Minimal inhibitory concentrations (MICs)

The minimum inhibitory concentrations (MICs) of 3',6-dinonyl neamine (Fig. 1) against different *S. aureus* strains were determined in comparison with those of amoxicillin, gentamicin, neomycin B, colistin and neamine (Table 1).

MICs of amoxicillin were very low (<0.025 and <0.25 µg/mL) on *S. aureus* ATCC 25923 and SA-1 respectively, intermediate on COL (4 µg/mL) and resistant on *S. aureus* ATCC33591, ATCC33592 and VRS2. Gentamicin showed low MICs (<0.125–2 µg/mL) on all bacterial species except for *S. aureus* VRS2 (64 µg/mL). Neomycin B was active against ATCC25923, COL and SA-1 strains (1 µg/mL) but ineffective against *S. aureus* ATCC33591, ATCC33592 and VRS2 (\geq 64 µg/mL). 3',6-Dinonyl neamine showed low MICs (1–2 µg/mL) on all bacterial species of *S. aureus* tested, including VRS2 towards gentamicin was inactive. Against *B. subtilis* (ATCC 6633), 3',6-dinonyl neamine also showed a low MIC value (1 µg/mL). Colistin and neamine, the parent compound of 3',6-dinonyl neamine, were inefficient with respect to all bacterial strains.

Table 1

Minimal inhibitory concentration against *S. aureus* (MSSA [ATCC 25923], MRSA [ATCC 33591, 33592, COL], SA-1-pump-NorA (expression of a fluor-quinolone-resistant efflux pump), VRS2 (vancomycin-resistant)).

Antibiotics	MICs <i>S. aureus</i> (μg/mL)					
	MSSA		MRSA		SA-1 pump NorA	VRS2
	ATCC 25923	ATCC 33591	ATCC 33592	COL		
Amoxicillin	<0.025	32	64	4	<0.25	64
Gentamicin	0.5	2	0.5	<0.125	1	64
Neomycin B	1	64	>64	0.25	1	64
Colistin	>128	>128	>128	>128	>128	>128
Neamine	8	>128	>128	32	>128	>128
3',6-Dinonyl neamine	1	1-2	2	1	1	1

3.2. Time killing curves

To elucidate the rate and extent of antibacterial activity and distinguish bacteriostatic from bactericidal antibiotics, time-kill assays were performed (Fig. 2).

In controls, the bacterial counts increased by 2.3 log₁₀ CFU/mL after 3 h. To compare the behavior of 3',6-dinonyl neamine to representative bactericidal and bacteriostatic antibiotics, experiments with gentamicin and linezolid respectively were conducted in parallel. With 3',6-dinonyl neamine, at 0.25 times the MIC, a delay in bacterial growth was observed. At the MIC, after 3 h, the ΔLog CFU (8 h-0 h) reached -1 with regrowth thereafter. At two and five times the MIC, ΔLog CFU (8 h-0 h) decreased to -3, -4. With 5 times the MIC, no bacteria were counted at 8 h. In comparison, with gentamicin at 0.25 times the MIC, the bacterial growth decreased. At 1, 2 and 5 times the MIC, gentamicin induced a huge reduction of the ΔLog CFU (8 h-0 h) to

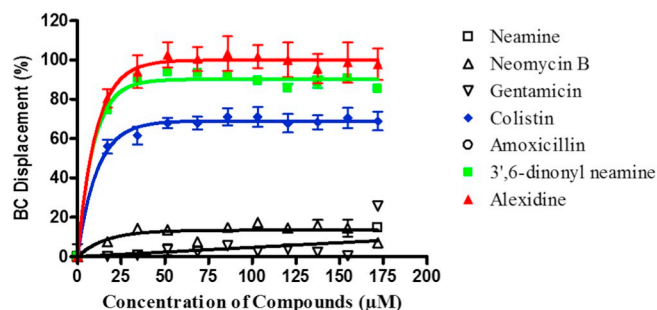


Fig. 3. Fluorescence of BODIPYTM-TR-cadaverine (BC) (5 μM). Displacement assay from cell free-LTA (3.5 μg/mL) by compounds of interest (Alexidine [Red triangles, ▲], 3',6-dinonyl neamine [Green squares, ■], Colistin [Blue diamonds, ◆], Neomycin B [Black open triangles, △], Gentamicin [Black open inverted triangles, ▽], Amoxicillin [Black open circles, ○], Neamine [Black open squares, □]). The data represent the mean ± SEM of three separate experiments.

-3, -4, after 3 h. Two hours later ΔLog CFU (8 h-0 h) reached -5 for gentamicin at 2 and 5 times MIC. With linezolid, at 0.25 times the MIC the bacterial growth was delayed. For higher concentrations (1, 2 and 5 times the MIC), a bacteriostatic effect was observed with the absence of bacterial growth. Very similar results are obtained with MRSA strain (ATCC 33592) for the 3 selected antibiotics.

The low MICs and the huge bactericidal effect of 3',6-dinonyl neamine against *S. aureus* MSSA and MRSA pushed us to investigate deeply the mechanism of action which could be responsible for these effects.

3.3. Binding affinity to lipoteichoic acids (LTA)

The mechanism of action of 3',6-dinonyl neamine was examined by studying its interaction with LTA from *S. aureus* using BODIPYTM-TR-

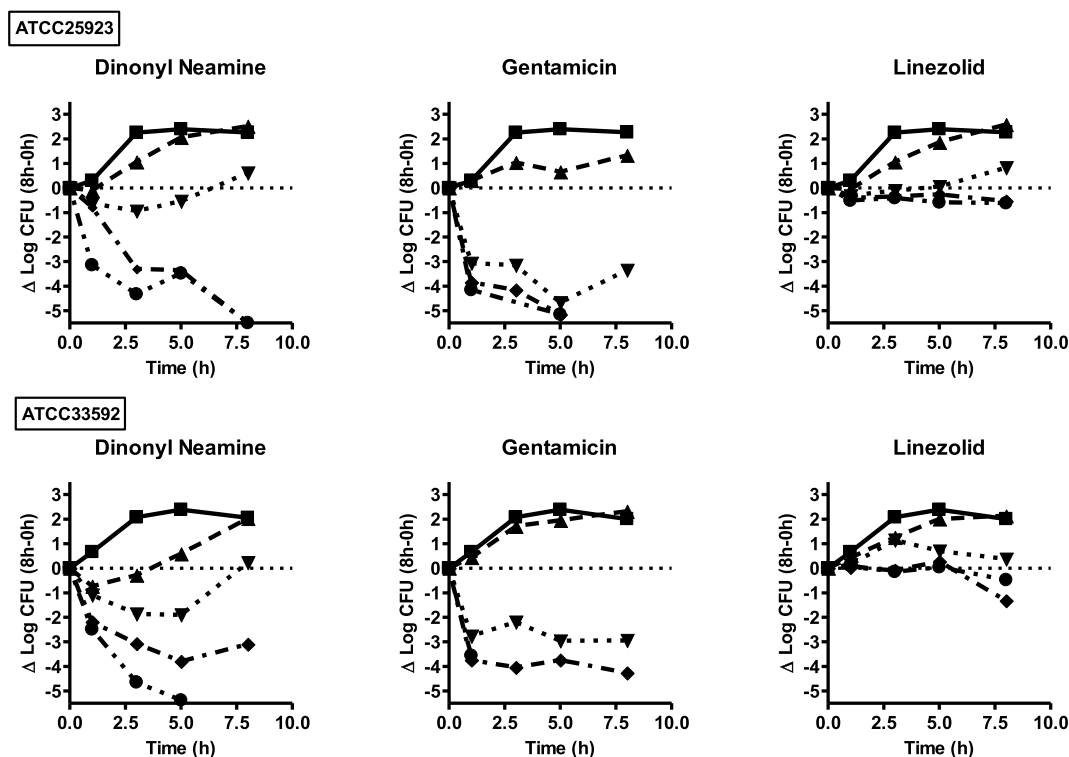


Fig. 2. Time-kill curves of 3',6-dinonyl neamine in comparison with gentamicin and linezolid against *S. aureus* ATCC 25923 and *S. aureus* MRSA (ATCC 33592). Exponentially growing *S. aureus* (■) was challenged with the test agents at 0.25 (▲), 1 (▼), 2 (◆) and 5 (●) times the MIC. Viability was enumerated at the indicated time points by serial dilution plating. Each point represents the mean of duplicate determinations. The limit of detection is a Δlog CFU of -5 (initial inoculum 10⁶ CFU/mL).

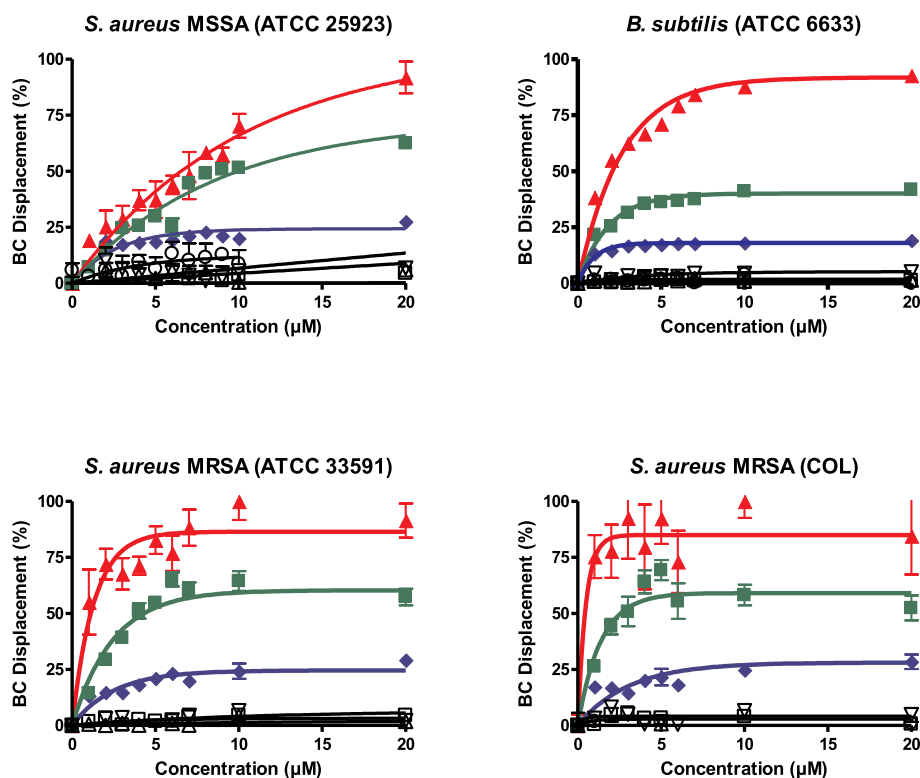


Fig. 4. BODIPY™-TR-cadaverine (BC) fluorescence as a reflection of BODIPY™-TR-cadaverine displacement from its binding to LTA of *S. aureus* (MSSA [ATCC 25923] and MRSA [ATCC 33591 and COL]) and *B. subtilis* (ATCC 6633) induced by increasing concentrations of selected compounds (Alexidine [Red triangles, ▲], 3',6-dinonyl neamine [Green squares, ■], Colistin [Blue diamonds, ◆], Neomycin B [Black open triangles, △], Gentamicin [Black open inverted triangles, ▽], Amoxicillin [Black open circles, ○], Neamine [Black open squares, □]). The data represent the mean ± SEM of three separate experiments.

cadaverine (BC) displacement assay. BODIPY™-TR-cadaverine is an amphiphilic molecule able to bind to LTA and undergo a quenching phenomenon of fluorescence. The binding of an exogenous molecule on cell free-LTA can be monitored by following the displacement of BODIPY™-TR-cadaverine from its binding to LTA as reflected by increase of the fluorescence intensity.

Fig. 3 shows the fluorescence data of BODIPY™-TR-cadaverine in cell free-LTA in presence of increasing concentrations of compounds of interest. Displacement of the BODIPY™-TR-cadaverine from cell free-LTA was observed with alexidine (positive control) and with 3',6-dinonyl neamine. Amoxicillin, neomycin B, gentamicin and neamine did not displace BODIPY™-TR-cadaverine from its binding to cell free-LTA. Colistin showed an intermediate behavior.

To know if 3',6-dinonyl neamine also binds to LTA at the surface of *S. aureus* and *B. subtilis*, we reproduced the BODIPY™-TR-cadaverine displacement assay on bacteria. Fig. 4 shows the evolution of the fluorescence of BODIPY™-TR-cadaverine reflecting displacement from its binding to *S. aureus* (MSSA [ATCC 25923] and MRSA [ATCC 33591, COL]) and *B. subtilis* (ATCC 6633) by different molecules of interest. Displacement of the BODIPY™-TR-cadaverine was observed in *S. aureus* and *B. subtilis*, through enhancement of fluorescence, ranking from alexidine, 3',6-dinonyl neamine and colistin. In contrast, neomycin B, gentamicin and neamine did not induce any displacement of BODIPY™-TR-cadaverine from *S. aureus* and *B. subtilis*, as expected.

These results suggest that the 3',6-dinonyl neamine binds with LTA of Gram-positive bacteria even some differences in the profile can be evidenced upon the strain. The extent of the effect with *S. aureus* is a little bit higher (around 55%) as compared to that observed with *B. subtilis* (around 35%). Regarding *S. aureus*, the effect of increasing concentrations of 3',6-dinonyl neamine with LTA seems more progressive for MSSA as compared with MRSA strains.

3.4. Effect on membrane potential

Beyond the interaction with surface component LTA, we investigated the effect of 3',6-dinonyl neamine on the membrane

potential of *S. aureus* (MSSA [ATCC 25923] and MRSA [ATCC 33591, COL]) and *B. subtilis* (ATCC 6633). For this purpose, we used DiSC₃(5), a marker whose fluorescence is dependent on the membrane potential. Based on the literature, valinomycin was used as a positive control [27].

Fig. 5 shows the fluorescence of DiSC₃(5) in the presence of 3',6-dinonyl neamine and other antibacterial drugs. Depolarization of the membrane of *S. aureus* and *B. subtilis* was observed with 3',6-dinonyl neamine and valinomycin. On *S. aureus*, as compared to the positive control, 3',6-dinonyl neamine induced changes in membrane potential in a more dependent fashion regarding the increase of concentrations. On *B. subtilis*, the effect is less progressive with the increase of 3',6-dinonyl neamine concentrations but also lower as compared to that observed with valinomycin even at the highest concentrations tested. With neomycin B, gentamicin, amoxicillin, neamine there was no or a limited effect on membrane potential, non-dependent upon the bacterial strains.

At a glance, in addition with its ability to bind to LTA, 3',6-dinonyl neamine induces membrane depolarization of Gram-positive bacteria.

3.5. Effects on membrane permeabilization

To investigate if binding of 3',6-dinonyl neamine to LTA and effect on membrane depolarization might result in bacterial membrane permeabilization, we used propidium iodide, a probe able to fluoresce when it binds to DNA. Since this probe is not capable to cross an intact lipid membrane it can bind to the DNA only if the membrane has been previously permeabilized. Based on the literature, alexidine was used as a positive control [32].

Fig. 6 shows the fluorescence of propidium iodide in the presence of different antibiotics. For both *S. aureus* and *B. subtilis*, permeabilization was observed after exposure to alexidine (positive control), 3',6-dinonyl neamine and colistin as revealed by the ranked increase of the intensity of propidium fluorescence. The effect induced by the amphiphilic neamine derivative was lower as compared to that observed with alexidine, even some variability in the extent of effect was showed

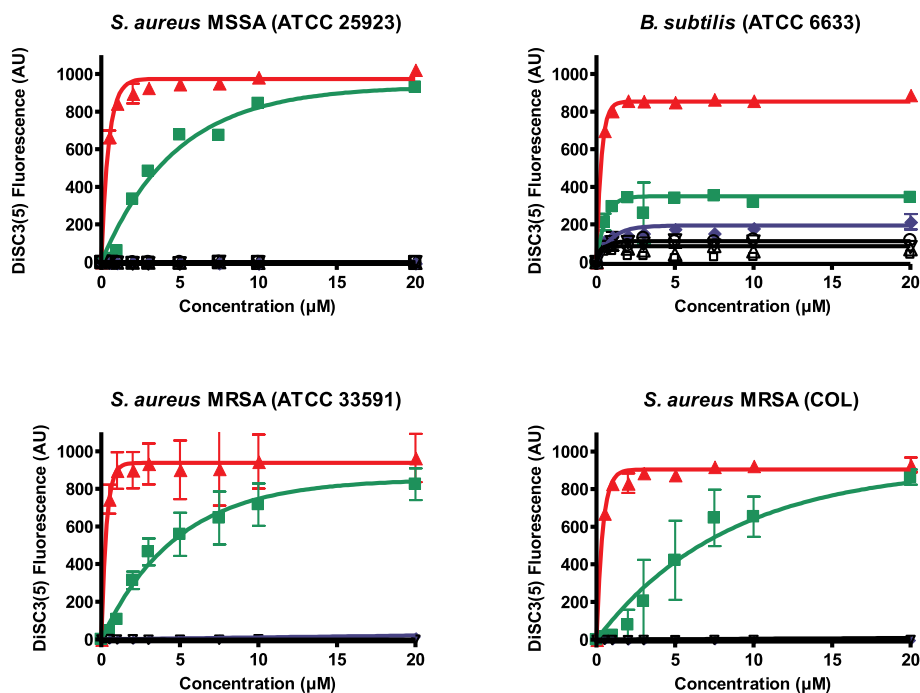


Fig. 5. DiSC3(5) fluorescence as a reflection of membrane potential of *S. aureus* (ATCC 25923, ATCC33591 and COL) and *B. subtilis* ATCC 6633. Increasing concentrations of selected compounds (Valinomycin [Red triangles, ▲], 3',6-dinonyl neamine [Green squares, ■], Colistin [Blue diamonds, ◆], Neomycin B [Black open triangles, △], Gentamicin [Black open inverted triangles, ▽], Amoxicillin [Black open circles, ○], Neamine [Black open squares, □]) were added and fluorescence intensity was recorded at 15 min. The data represent the mean ± SEM of three separate experiments.

depending upon the strain. No permeabilization was observed with the other molecules tested, e.g. neomycin B, gentamicin, amoxicillin, and neamine.

Thus 3',6-dinonyl neamine is able to efficiently permeabilize the bacterial membranes of *S. aureus* and *B. subtilis*.

3.6. Effects on bacterial morphology and lipid distribution

The effects of 3',6-dinonyl neamine on morphology of bacteria was first examined by electron microscopy imaging. Fig. 6 shows the electron microscopy images of *S. aureus* (spherical shape) and *B. subtilis* (rod shape) with or without exposition of 3',6-dinonyl neamine (2 MIC;

2 µM) for 30 min. Huge morphological changes were observed for both pathogens including cell damages and deformations of cell membrane. The appearance of *S. aureus* in the absence of drug is shown in Fig. 7 (top, left). The bacteria were smooth and rounded. The organisms were grouped in characteristic grapelike clusters. After exposure to 3',6-dinonyl neamine, morphological alterations with cell collapse were evidenced (Fig. 7, top, right). On *B. subtilis*, an effect of 3',6-dinonyl neamine (Fig. 7, bottom, right) was also observed as numerous damaged cells in comparison to the control (Fig. 7, bottom, left). A shift from the normal rod shape to that of a bent rod, and swelling into irregular shapes was evidenced.

We next investigated the potential consequence of membrane

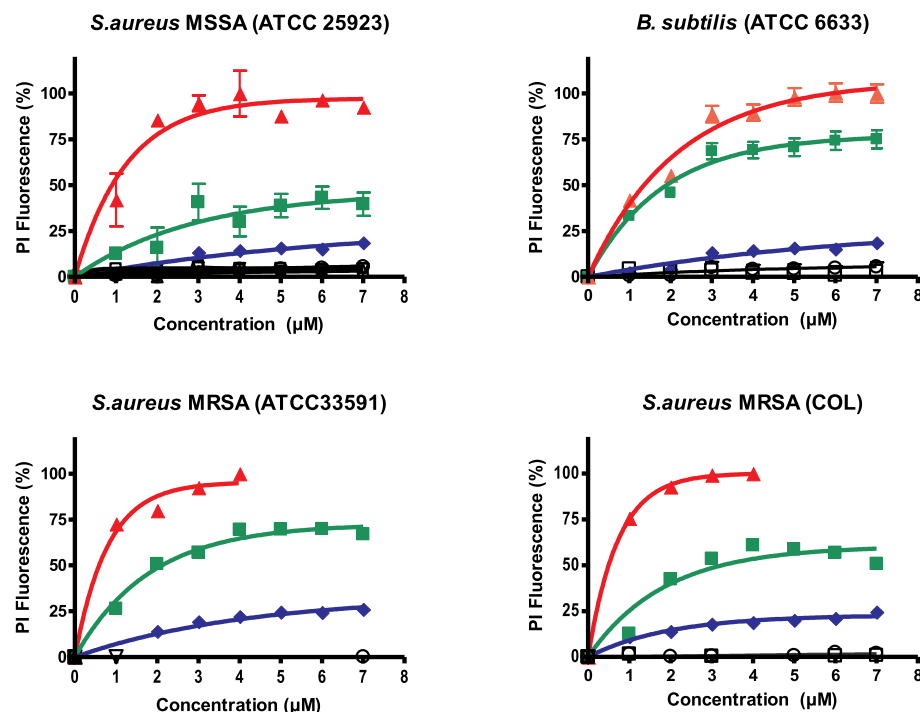


Fig. 6. Propidium iodide fluorescence as a reflection of membrane permeabilization of *S. aureus* ATCC 25923 (left) and *B. subtilis* ATCC 6633 (right) treated with increasing concentrations of selected compounds. (Alexidine [Red triangles, ▲], 3',6-dinonyl neamine [Green squares, ■], Colistin [Blue diamonds, ◆], Neomycin B [Black open triangles, △], Gentamicin [Black open inverted triangles, ▽], Amoxicillin [Black open circles, ○], Neamine [Black open squares, □]). The data represent the mean ± SEM of three separate experiments.

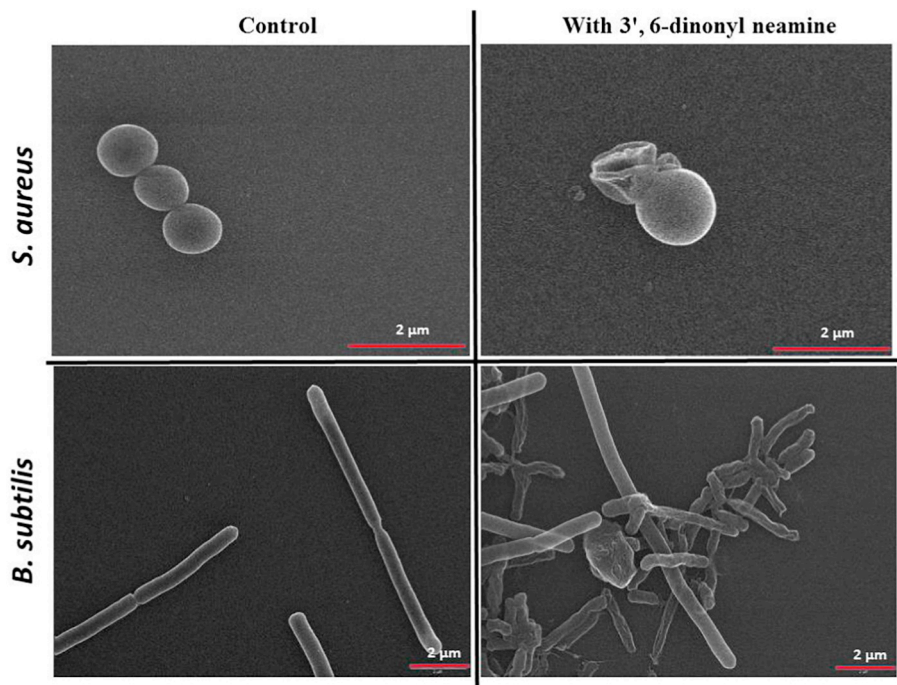


Fig. 7. SEM images of the effect of 3',6-dinonyl neamine on the morphology of *S. aureus* ATCC 25923 (Top) and *B. subtilis* ATCC 6633 (Bottom). The concentration of 3',6-dinonyl neamine used is 2 μM, (2 times the MIC) and the incubation time was 30 min. Scale bars correspond to 2 μm. Images were representative of >200 pictures.

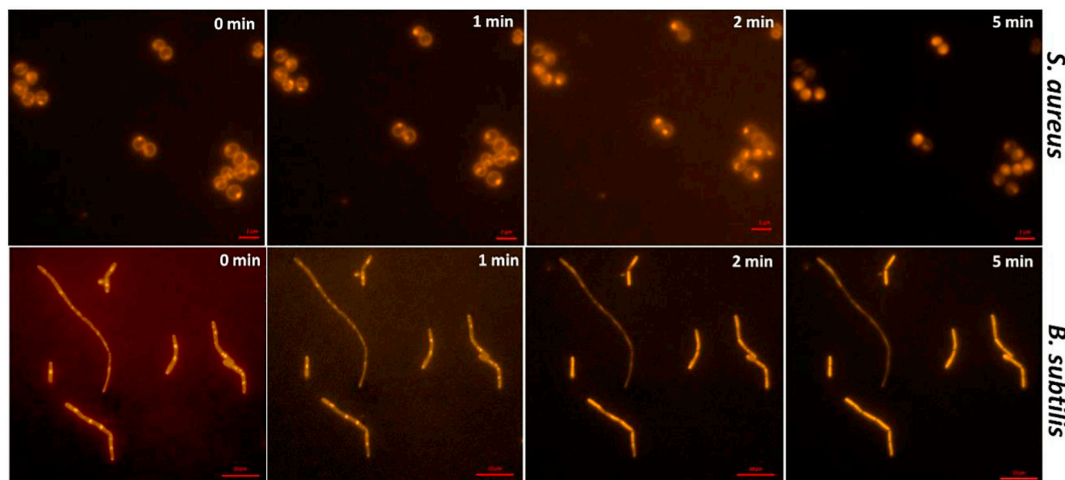


Fig. 8. Time lapsed Nile red fluorescence images of *S. aureus* ATCC 25923 and *B. subtilis* ATCC 6633. The concentration of 3',6-dinonyl neamine used is 2 * MIC. Scale bars correspond to 10 μm.

depolarization induced by 3',6-dinonyl neamine, on Nile Red fluorescence. Nile Red is an uncharged fluorescent dye that partitions into lipid membranes based on its intrinsic hydrophobicity [31,33] and fluidity of the membrane [30]. *S. aureus* and *B. subtilis* were labelled with Nile Red, and time lapsed images are taken at room temperature after incubation with the 3',6-dinonyl neamine at 2 times the MIC (Fig. 8). We observed a stronger fluorescence signal at division septa, which is caused by the presence of two adjacent cell membranes where the newly daughter cells are formed. When compared to control cells (time 0), an overall changes in fluorescence distribution in cells was detected with a more homogeneous labelling as clearly illustrated on *B. subtilis* after 2–5 min. The membrane staining effects were already visible within 2 min after the addition of the neamine derivative (2 MIC), suggesting these changes were not formed by accumulation of newly synthesized membrane material.

To get more insight on what are the effects of the 3',6-dinonyl neamine on *S. aureus*, we explored the potential effect of this derivative on the localization of PBP2, a septum-localized protein involved in *S. aureus* cell division. We used a GFP-PBP2 fusion in MRSA strain COL (Fig. 9). In untreated *S. aureus*, PBP2 preferentially localized at the septum (see arrows), while the addition of 3',6-dinonyl neamine caused its redistribution with very few bacteria labelled at the septum (see arrows) suggesting impairment of the new peptidoglycan synthesis at the cell division site and/or inhibition of septum formation [34].

4. Discussion

Bacterial membrane geometry has recently been recognized as an important determinant for both lipid and protein localization. If the mechanism of protein localization is both conserved and essential in

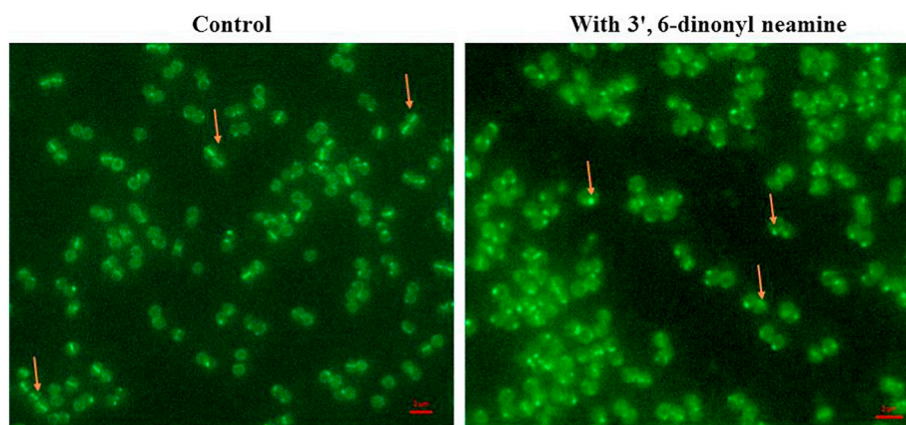


Fig. 9. Fluorescence images of GFP-tagged PBP2 of *S. aureus* COL strain. The concentration of 3',6-dinonyl neamine used was 1 * MIC and time of incubation, 30 min. Scale bars correspond to 2 μ m.

bacteria, it is possible that some antibiotics may have evolved to exploit it as a novel target. Here, we aimed to investigate if 3',6-dinonyl neamine is able to interact with lipid membranes of Gram-positive bacteria, modify their biophysical properties with potential impacts of proteins depending upon lipids for their proper activity.

On *S. aureus* and *B. subtilis*, we demonstrated the bactericidal activity of 3',6-dinonyl neamine. Focusing on the molecular mechanism of action, we showed this amphiphilic neamine derivative interacts with the bacterial surface lipoteichoic acids (LTA), disrupts the membrane potential and enhances the membrane permeability. By imaging, we illustrated the ability of 3',6-dinonyl neamine to induce changes in lipid organization reflecting MreB location and to interfere with the formation of septum. In turn this could impair the synthesis of new peptidoglycan at the cell division site. Altogether, the mechanism of action of 3',6-dinonyl neamine against Gram-positive could be viewed in three major steps.

The first event is the interaction of the 3',6-dinonyl neamine with LTA. LTA from *S. aureus* is made of polyglycerophosphate (poly-GroP) repeats anchored directly to the cell membrane via a diacylglycerol-gentiobiose moiety [17,35]. This is an anionic polymer that can bind the positively-charged amphiphilic neamine derivative. If LTA act as an entrainer or ladder for a route to the cytoplasmic membrane is still unknown. Concentrations and structure of the amphiphilic antibacterial, and the lipid composition of cytoplasmic membrane are probably critical for deciphering if bacterial cell wall components, peptidoglycan and lipoteichoic acids, serve as electrostatic barriers capturing the 3',6-dinonyl neamine and in turn preventing their interaction with the cytoplasmic membrane or attract the compound to allow to reach the cytoplasmic membranes. The latter is probably the right process since 3',6-dinonyl neamine induces membrane depolarization, permeabilization and changes in lipid organization. The differences we observed between the ability of the 3',6-dinonyl neamine to displace the BODIPYTM-TR cadaverine from its binding to LTA of *S. aureus* or *B. subtilis* could result from differences in mechanisms involved in glycosylation of wall teichoic acids in Gram-positive bacteria [36], and esterification of the glycerolphosphate subunits leading to a varying degree in D-alanine groups [17,37,38]. How GlcNAcylation and/or D-alanine modification impacts LTA structure and function is still unknown but this could result from differences in surface electrostatics, cell membrane fluidity and conformation of LTA as well as potencies in the stimulation of TLR2 of Gram-positive bacteria [39].

The second event would be the interaction with cytoplasmic membrane a process probably highly dependent upon its composition. *S. aureus*, contains about 55% of negatively-charged PG [16]. In contrast, the membrane of *B. subtilis* is composed of about 70 mol% of PG [40,41]. In addition, both types of bacteria have about 5% negatively-charged and negative curvature strain-inducing cardiolipin [15,42].

The higher content of negatively-charged lipids in the membrane of *B. subtilis* might drive electrostatic interactions and favor amphiphilic neamine derivative accumulation on the bacterial surface [15]. Preferred binding to membrane regions with high curvature which are rich in cardiolipin microdomains and in phosphatidylethanolamine might additionally contribute to the distinct distribution of amphiphilic neamine observed in rod-shaped *B. subtilis* cells [41,43–45]. However, other parameters are probably involved since we observed a lower effect induced by 3',6-dinonyl neamine on the displacement of BodipyTM-TR-cadaverine from binding to LTA or on membrane depolarization with *B. subtilis* as compared with *S. aureus*. Additional questions were also raised regarding the mechanism involved in membrane depolarization induced by 3',6-dinonyl neamine. It probably results from the formation of pore in the cytoplasmic membrane as it has been described for nisin [46]. However, rather than depolarizing the membrane through bilayer perturbation, the observed gradual reduction of membrane potential could also be due to the specific inhibition of the respiratory chain. In addition, possible dissociation between membrane depolarisation and direct membrane permeabilization can occur as observed on *B. subtilis* [47].

The third step would be changes in protein activity as, in part, the result from drug/lipid interaction. Many proteins involved in the regulation and maintenance of bacterial growth reside in the cytoplasmic membrane and are dependent upon lipids. The division site appears to be enriched for certain phospholipids, including cardiolipin to which the 3',6-dinonyl neamine is able to bind [12,13]. This suggests a role of the lipid composition at the septum for the assembly and maintenance of the biosynthetic machinery. From our results, and based on the relation between the Nile Red fluorescence and MreB localization [29] we first suggest that 3',6-dinonyl neamine might induce a potential effect on MreB location on *S. aureus* and *B. subtilis*. In turn, this could impair peptidoglycan synthesis since MreB forms a complex with the conserved membrane proteins MreC and MreD, and with proteins involved in peptidoglycan synthesis such as RodA, MurG, MraY, and several penicillin binding proteins (PBPs) [48–50]. A second feature from this work is the ability of the 3',6-dinonyl neamine to impair the formation of the septum, as demonstrated by imaging the fluorescence of GFP-PBP2 in *S. aureus*. PBP2 is a penicillin binding protein recruited to the septum by a process requiring the presence of FtsZ, a protein that anchors the cell wall synthetic machinery to the site of cell division [34,34]. More experiments are required to ascertain if there is a delocalization of PBP2 from the FtsZ-anchored cell wall biosynthetic machinery at the septal division site as demonstrated for the FtsZ-targeting agent (TXA707) [51], ursolic acid [52], and epicatechin gallate [53]. Additional studies are also required to fully understand the coordination of cell wall synthesis and cell constriction, two processes highly interconnected and requiring the interplay of dozens of proteins [54].

Among those proteins, it would be interesting to focus on FtsZ/FtsA (FtsAZ) and DivA. FtsAZ filaments treadmilled circumferentially around the division ring, driving the motions of the peptidoglycan synthesizing enzymes and cell division [54]. DivIVA is involved in cell division protein and its recruitment leads to local changes in peptidoglycan biogenesis, including localized inhibition of lateral cell wall biosynthesis. DivIVA [55–57], localizes principally as a ring at nascent septa and secondarily to the less negatively curved, inside surface of the hemispherical poles of *B. subtilis* [57]. Since it recognizes the localized region of membrane distortion and altered curvature [11,56,57], amphiphilic aminoglycoside derivatives which have a large headgroup volume and a short, small-volume tail could produce local alterations in membrane curvature and impair DivIVA.

All together these three steps are closely linked. The potential defect in the formation/characteristics of LTA resulting from the binding of 3',6-dinonyl neamine might lead to shape malformations and to impaired septation and cell division. However, how localization of LTA synthesis proteins is co-ordinate to proteins involved in the cell division machinery [58,59] should be addressed.

From a microbiological point of view, we did not observe any major difference in the effect of 3',6-dinonyl neamine on *S. aureus* MSSA (ATCC 29523) and MRSA (ATCC 33591, COL) if we compare its ability to displace the Bodipy™-TR-cadaverine from its binding to LTA, as well as to depolarize and permeabilize the bacterial cytoplasmic membrane. At a first glance, it could be surprising taking into differences in genetic patterns as well as morphological changes including the greater thickness of the wall or septum for MRSA [60]. From a clinical point of view, this can however viewed as a great advantage to have antibiotic active against a large panel of strains including resistant ones.

At a glance, we showed that 3',6-dinonyl neamine, an amphiphilic neamine derivative already described for its interest against Gram-negative bacteria including resistant *P. aeruginosa* [7], is also active on Gram-positive bacteria including *S. aureus* MRSA. By time killing curves, we assessed the bactericidal effect induced by 3',6-dinonyl neamine on *S. aureus* MSSA and MRSA. Moreover, we demonstrated the ability of 3',6-dinonyl neamine to interact with the surface components (LTA) of Gram-positive bacteria, to induce membrane depolarization, and to enhance membrane permeabilization. At the septum, the amphiphilic derivative of neamine induced changes in lipid-enriched region of *S. aureus* and *B. subtilis*, and impaired the formation of the septum. These multiple effects related to different potential targets should lead to the development of new promising agents able to fight the increase of bacterial resistance to current antibiotics.

Transparency document

The [Transparency document](#) associated with this article can be found, in online version.

Acknowledgments

This work was supported by «Fonds de la Recherche Scientifique Médicale» (grants T.1003.14 and J.0205.16), «Fondation pour la Recherche Médicale» (post-doctoral grant for CD, DBF20161136768), SATT Linksum Grenoble Alpes and Labex ARCANE and CBH-EUR-GS (ANR-17-EURE-0003). We thank for providing us with strains the Network on Antimicrobial Resistance in *S. aureus* (MRSA and VRS2; Eurofins Medinet Inc., Hendon, VA). We also thank L. Catteau for critical reading and V. Mohymont and Vasileios Yfantis for providing dedicated technical assistance for cell studies.

References

- [1] C.S. Lopez, A.F. Alice, H. Heras, E.A. Rivas, C. Sanchez-Rivas, Role of anionic phospholipids in the adaptation of *Bacillus subtilis* to high salinity, *Microbiology* 152 (2006) 605–616 Pt 3.
- [2] H. Vitrac, D.M. MacLean, V. Jayaraman, M. Bogdanov, W. Dowhan, Dynamic membrane protein topological switching upon changes in phospholipid environment, *Proc. Natl. Acad. Sci. U. S. A.* 112 (45) (2015) 13874–13879.
- [3] R.M. Epanand, C. Walker, R.F. Epanand, N.A. Magarvey, Molecular mechanisms of membrane targeting antibiotics, *Biochim. Biophys. Acta* 1858 (5) (2016) 980–987.
- [4] K. Bush, Antimicrobial agents targeting bacterial cell walls and cell membranes, *Rev. Sci. Tech.* 31 (1) (2012) 43–56.
- [5] I. Baussanne, A. Bussiere, S. Halder, C. Ganem-Elbaz, M. Ouberai, M. Riou, J.M. Paris, E. Ennifar, M.P. Mingeot-Leclercq, J.L. Decout, Synthesis and antimicrobial evaluation of amphiphilic neamine derivatives, *J. Med. Chem.* 53 (1) (2010) 119–127.
- [6] O. Jackowski, A. Bussière, C. Vanhaverbeke, I. Baussanne, E. Peyrin, M.P. Mingeot-Leclercq, J.L. Decout, Major increases of the reactivity and selectivity in aminoglycoside O-alkylation due to the presence of fluoride ions, *Tetrahedron* 68 (2012) 737–746.
- [7] L. Zimmermann, I. Das, J. Desire, G. Sautrey, R.S.V. Barros, K.M. El, M.P. Mingeot-Leclercq, J.L. Decout, New broad-spectrum antibacterial amphiphilic aminoglycosides active against resistant bacteria: from neamine derivatives to smaller neosamine analogues, *J. Med. Chem.* 59 (20) (2016) 9350–9369.
- [8] L. Zimmermann, A. Bussiere, M. Ouberai, I. Baussanne, C. Jolival, M.P. Mingeot-Leclercq, J.L. Decout, Tuning the antibacterial activity of amphiphilic neamine derivatives and comparison to paromamine homologues, *J. Med. Chem.* 56 (19) (2013) 7691–7705.
- [9] L. Zimmermann, J. Kempf, F. Brie, J. Swain, M.P. Mingeot-Leclercq, J.L. Decout, Broad-spectrum antibacterial amphiphilic aminoglycosides: a new focus on the structure of the lipophilic groups extends the series of active dialkyl neamines, *Eur. J. Med. Chem.* 157 (2018) 1512–1525.
- [10] M. Ouberai, G.F. El, A. Bussiere, M. Riou, D. Alsteens, L. Lins, I. Baussanne, Y.F. Dufrene, R. Brasseur, J.L. Decout, M.P. Mingeot-Leclercq, The *Pseudomonas aeruginosa* membranes: a target for a new amphiphilic aminoglycoside derivative? *Biochim. Biophys. Acta* 1808 (6) (2011) 1716–1727.
- [11] G. Sautrey, L. Zimmermann, M. Deleu, A. Delbar, M.L. Souza, K. Jeannot, B.F. Van, J.M. Buyck, J.L. Decout, M.P. Mingeot-Leclercq, New amphiphilic neamine derivatives active against resistant *Pseudomonas aeruginosa* and their interactions with lipopolysaccharides, *Antimicrob. Agents Chemother.* 58 (8) (2014) 4420–4430.
- [12] G. Sautrey, K.M. El, A.G. Dos Santos, L. Zimmermann, M. Deleu, L. Lins, J.L. Decout, M.P. Mingeot-Leclercq, Negatively charged lipids as a potential target for new amphiphilic aminoglycoside antibiotics: a biophysical study, *J. Biol. Chem.* 291 (26) (2016) 13864–13874.
- [13] M. El Khoury, J. Swain, G. Sautrey, L. Zimmermann, P. Van Der Smisen, R.F. Decout, M.P. Mingeot-Leclercq, Targeting bacterial cardiolipin enriched microdomains: an antimicrobial strategy used by amphiphilic aminoglycoside antibiotics, *Sci. Rep.* 7 (1) (2017) 10697.
- [14] N. Malanovic, K. Lohner, Gram-positive bacterial cell envelopes: the impact on the activity of antimicrobial peptides, *Biochim. Biophys. Acta* 1858 (5) (2016) 936–946.
- [15] R.M. Epanand, R.F. Epanand, Domains in bacterial membranes and the action of antimicrobial agents, *Mol. Biosyst.* 5 (6) (2009) 580–587.
- [16] R.M. Epanand, R.F. Epanand, Bacterial membrane lipids in the action of antimicrobial agents, *J. Pept. Sci.* 17 (5) (2011) 298–305.
- [17] M.G. Percy, A. Grundling, Lipoteichoic acid synthesis and function in gram-positive bacteria, *Annu. Rev. Microbiol.* 68 (2014) 81–100.
- [18] H.F. Chambers, F.R. Deleo, Waves of resistance: *Staphylococcus aureus* in the antibiotic era, *Nat. Rev. Microbiol.* 7 (9) (2009) 629–641.
- [19] J.D. Nickels, S. Chatterjee, C.B. Stanley, S. Qian, X. Cheng, D.A.A. Myles, R.F. Standaert, J.G. Elkins, J. Katsaras, The in vivo structure of biological membranes and evidence for lipid domains, *PLoS Biol.* 15 (5) (2017) e2002214.
- [20] R.M. Figge, A.V. Divakaruni, J.W. Gober, MreB, the cell shape-determining bacterial actin homologue, co-ordinates cell wall morphogenesis in *Caulobacter crescentus*, *Mol. Microbiol.* 51 (5) (2004) 1321–1332.
- [21] P. Arede, J. Ministro, D.C. Oliveira, Redefining the role of the beta-lactamase locus in methicillin-resistant *Staphylococcus aureus*: beta-lactamase regulators disrupt the MecI-mediated strong repression on *mecA* and optimize the phenotypic expression of resistance in strains with constitutive *mecA* expression, *Antimicrob. Agents Chemother.* 57 (7) (2013) 3037–3045.
- [22] L.H. De, S.W. Wu, M.G. Pinho, A.M. Ludovice, S. Filipe, S. Gardete, R. Sobral, S. Gill, M. Chung, A. Tomasz, Antibiotic resistance as a stress response: complete sequencing of a large number of chromosomal loci in *Staphylococcus aureus* strain COL that impact on the expression of resistance to methicillin, *Microb. Drug Resist.* 5 (3) (1999) 163–175.
- [23] C.M. Tan, A.G. Therien, J. Lu, S.H. Lee, A. Caron, C.J. Gill, C. Lebeau-Jacob, L. Benton-Perdomo, J.M. Monteiro, P.M. Pereira, N.L. Elsen, J. Wu, K. Deschamps, M. Petcu, S. Wong, E. Daignault, S. Kramer, L. Liang, E. Maxwell, D. Claveau, J. Vaillancourt, K. Skorey, J. Tam, H. Wang, T.C. Meredith, S. Sillaots, L. Wang-Jarantow, Y. Ramtohol, E. Langlois, F. Landry, J.C. Reid, G. Parthasarathy, S. Sharma, A. Baryshnikova, K.J. Lumb, M.G. Pinho, S.M. Soisson, T. Roemer, Restoring methicillin-resistant *Staphylococcus aureus* susceptibility to beta-lactam antibiotics, *Sci. Transl. Med.* 4 (126) (2012) 126ra35.
- [24] J.C. Haught, S. Xie, B. Circello, C.S. Tansky, D. Khambe, Y. Sun, Y. Lin, K. Sreekrishna, M. Klukowska, T. Huggins, D.J. White, Lipopolysaccharide and lipoteichoic acid binding by antimicrobials used in oral care formulations, *Am. J. Dent.* 29 (6) (2016) 328–332.
- [25] S.J. Wood, K.A. Miller, S.A. David, Anti-endotoxin agents. 1. Development of a fluorescent probe displacement method optimized for the rapid identification of lipopolysaccharide-binding agents, *Comb. Chem. High Throughput Screen.* 7 (3) (2004) 239–249.

- [26] S. Krasne, Interactions of voltage-sensing dyes with membranes. I. Steady-state permeability behaviors induced by cyanine dyes, *Biophys. J.* 30 (3) (1980) 415–439.
- [27] J.D. Te Winkel, D.A. Gray, K.H. Seistrup, L.W. Hamoen, H. Strahl, Analysis of antimicrobial-triggered membrane depolarization using voltage sensitive dyes, *Front Cell Dev. Biol.* 4 (2016) 29.
- [28] G.W. Niven, F. Mulholland, Cell membrane integrity and lysis in *Lactococcus lactis*: the detection of a population of permeable cells in post-logarithmic phase cultures, *J. Appl. Microbiol.* 84 (1) (1998) 90–96.
- [29] H. Strahl, F. Burmann, L.W. Hamoen, The actin homologue MreB organizes the bacterial cell membrane, *Nat. Commun.* 5 (2014) 3442.
- [30] O.A. Kucherak, S. Oncul, Z. Darwich, D.A. Yushchenko, Y. Arntz, P. Didier, Y. Mely, A.S. Klymchenko, Switchable Nile red-based probe for cholesterol and lipid order at the outer leaflet of biomembranes, *J. Am. Chem. Soc.* 132 (13) (2010) 4907–4916.
- [31] P. Greenspan, S.D. Fowler, Spectrofluorometric studies of the lipid probe, Nile red, *J. Lipid Res.* 26 (7) (1985) 781–789.
- [32] W. Sianglum, D. Saeloh, P. Tongtawe, N. Wootipoom, N. Indrawattana, S.P. Voravuthikunchai, Early effects of rhodomlyrtone on membrane integrity in methicillin-resistant *Staphylococcus aureus*, *Microb. Drug Resist.* 24 (7) (2018) 882–889.
- [33] S. Mukherjee, H. Raghuraman, A. Chattopadhyay, Membrane localization and dynamics of Nile Red: effect of cholesterol, *Biochim. Biophys. Acta* 1768 (1) (2007) 59–66.
- [34] M.G. Pinho, J. Errington, Recruitment of penicillin-binding protein PBP2 to the division site of *Staphylococcus aureus* is dependent on its transpeptidation substrates, *Mol. Microbiol.* 55 (3) (2005) 799–807.
- [35] A. Grundling, O. Schneewind, Genes required for glycolipid synthesis and lipoteichoic acid anchoring in *Staphylococcus aureus*, *J. Bacteriol.* 189 (6) (2007) 2521–2530.
- [36] J. Rismondo, M.G. Percy, A. Grundling, Discovery of genes required for lipoteichoic acid glycosylation predicts two distinct mechanisms for wall teichoic acid glycosylation, *J. Biol. Chem.* 293 (9) (2018) 3293–3306.
- [37] W. Fischer, P. Rosel, The alanine ester substitution of lipoteichoic acid (LTA) in *Staphylococcus aureus*, *FEBS Lett.* 119 (2) (1980) 224–226.
- [38] B.M. Wood, J.P.J. Santa Maria, L.M. Matano, C.R. Vickery, S. Walker, A partial reconstitution implicates DltD in catalyzing lipoteichoic acid d-alanylation, *J. Biol. Chem.* 293 (46) (2018) 17985–17996.
- [39] Y.H. Ryu, J.E. Baik, J.S. Yang, S.S. Kang, J. Im, C.H. Yun, D.W. Kim, K. Lee, D.K. Chung, H.R. Ju, S.H. Han, Differential immunostimulatory effects of Gram-positive bacteria due to their lipoteichoic acids, *Int. Immunopharmacol.* 9 (1) (2009) 127–133.
- [40] J.A. den Kamp, I. Redai, L.L. van Deenen, Phospholipid composition of *Bacillus subtilis*, *J. Bacteriol.* 99 (1) (1969) 298–303.
- [41] F. Kawai, M. Shoda, R. Harashima, Y. Sadaie, H. Hara, K. Matsumoto, Cardiolipin domains in *Bacillus subtilis* marburg membranes, *J. Bacteriol.* 186 (5) (2004) 1475–1483.
- [42] K. Matsumoto, J. Kusaka, A. Nishibori, H. Hara, Lipid domains in bacterial membranes, *Mol. Microbiol.* 61 (5) (2006) 1110–1117.
- [43] E. Mileykovskaya, W. Dowhan, R.L. Birke, D. Zheng, L. Lutterodt, T.H. Haines, Cardiolipin binds nonyl acridine orange by aggregating the dye at exposed hydrophobic domains on bilayer surfaces, *FEBS Lett.* 507 (2) (2001) 187–190.
- [44] T. Zhang, J.K. Muraih, N. Tishbi, J. Herskowitz, R.L. Victor, J. Silverman, S. Uwumarenogie, S.D. Taylor, M. Palmer, E. Mintzer, Cardiolipin prevents membrane translocation and permeabilization by daptomycin, *J. Biol. Chem.* 289 (17) (2014) 11584–11591.
- [45] D.E. Minnikin, H. Abdolrahimzadeh, J. Baddiley, The occurrence of phosphatidylethanolamine and glycosyl diglycerides in thermophilic bacilli, *J. Gen. Microbiol.* 83 (2) (1974) 415–418.
- [46] J. Medeiros-Silva, S. Jekhmene, A.L. Paioni, K. Gawarecka, M. Baldus, E. Swiezewska, E. Breukink, M. Weingarth, High-resolution NMR studies of antibiotics in cellular membranes, *Nat. Commun.* 9 (1) (2018) 3963.
- [47] A. Muller, M. Wenzel, H. Strahl, F. Grein, T.N.V. Saaki, B. Kohl, T. Siersma, J.E. Bandow, H.G. Sahl, T. Schneider, L.W. Hamoen, Daptomycin inhibits cell envelope synthesis by interfering with fluid membrane microdomains, *Proc. Natl. Acad. Sci. U. S. A.* 113 (45) (2016) E7077–E7086.
- [48] P.V. Olshausen, H.J. Defeu Soufo, K. Wicker, R. Heintzmann, P.L. Graumann, A. Rohrbach, Superresolution imaging of dynamic MreB filaments in *B. subtilis*—a multiple-motor-driven transport? *Biophys. J.* 105 (5) (2013) 1171–1181.
- [49] W. Margolin, Sculpting the bacterial cell, *Curr. Biol.* 19 (17) (2009) R812–R822.
- [50] T. Mohammadi, A. Karczmarek, M. Crouvoisier, A. Bouhss, D. Mengin-Lecreux, B.T. den, The essential peptidoglycan glycosyltransferase MurG forms a complex with proteins involved in lateral envelope growth as well as with proteins involved in cell division in *Escherichia coli*, *Mol. Microbiol.* 65 (4) (2007) 1106–1121.
- [51] E. Ferrer-Gonzalez, M. Kaul, A.K. Parhi, E.J. LaVoie, D.S. Pilch, Beta-lactam antibiotics with a high affinity for PBP2 act synergistically with the FtsZ-targeting agent TXA707 against methicillin-resistant *Staphylococcus aureus*, *Antimicrob. Agents Chemother.* 61 (9) (2017).
- [52] L. Cateau, N.T. Reichmann, J. Olson, M.G. Pinho, V. Nizet, B.F. Van, J. Quetin-Leclercq, Synergy between ursolic and oleanolic acids from *Vitellaria paradoxa* leaf extract and beta-lactams against methicillin-resistant *Staphylococcus aureus*: in vitro and in vivo activity and underlying mechanisms, *Molecules.* 22 (12) (2017).
- [53] P. Bernal, S. Lemaire, M.G. Pinho, S. Mobashery, J. Hinds, P.W. Taylor, Insertion of epicatechin gallate into the cytoplasmic membrane of methicillin-resistant *Staphylococcus aureus* disrupts penicillin-binding protein (PBP) 2a-mediated beta-lactam resistance by delocalizing PBP2, *J. Biol. Chem.* 285 (31) (2010) 24055–24065.
- [54] A.W. Bisson-Filho, Y.P. Hsu, G.R. Squyres, E. Kuru, F. Wu, C. Jukes, Y. Sun, C. Dekker, S. Holden, M.S. VanNieuwenhze, Y.V. Brun, E.C. Garner, Treadmilling by FtsZ filaments drives peptidoglycan synthesis and bacterial cell division, *Science* 355 (6326) (2017) 739–743.
- [55] P. Eswaramoorthy, M.L. Erb, J.A. Gregory, J. Silverman, K. Pogliano, J. Pogliano, K.S. Ramamurthi, Cellular architecture mediates DivIVA ultrastructure and regulates min activity in *Bacillus subtilis*, *MBio.* 2 (6) (2011).
- [56] R. Lenarcic, S. Halbedel, L. Visser, M. Shaw, L.J. Wu, J. Errington, D. Marenduzzo, L.W. Hamoen, Localisation of DivIVA by targeting to negatively curved membranes, *EMBO J.* 28 (15) (2009) 2272–2282.
- [57] K.S. Ramamurthi, R. Losick, Negative membrane curvature as a cue for subcellular localization of a bacterial protein, *Proc. Natl. Acad. Sci. U. S. A.* 106 (32) (2009) 13541–13545.
- [58] K. Schirmer, J. Marles-Wright, R.J. Lewis, J. Errington, Distinct and essential morphogenic functions for wall- and lipo-teichoic acids in *Bacillus subtilis*, *EMBO J.* 28 (7) (2009) 830–842.
- [59] N.T. Reichmann, C.C. Picarra, J.M. Monteiro, A.L. Bottomley, R.M. Corrigan, S.J. Foster, M.G. Pinho, A. Grundling, Differential localization of LTA synthesis proteins and their interaction with the cell division machinery in *Staphylococcus aureus*, *Mol. Microbiol.* 92 (2) (2014) 273–286.
- [60] A.B. Garcia, J.M. Vinuela-Prieto, L. Lopez-Gonzalez, F.J. Candel, Correlation between resistance mechanisms in *Staphylococcus aureus* and cell wall and septum thickening, *Infect. Drug Resist.* 10 (2017) 353–356.